EFFECT OF SOL CONCENTRATION AND SUBSTRATE TYPE ON MICROSTRUCTURE FORMATION OF PZT THIN FILMS

HELENA BRUNCKOVÁ, ĽUBOMÍR MEDVECKÝ

Institute of Materials Research, Slovak Academy of Sciences, Watsonova 47, 040 01 Košice, Slovak Republic

E-mail: hbrunckova@imr.saske.sk

Submitted June 11, 2010; accepted January 20, 2011

Keywords: Sol-gel, PZT thin films, Spin-coating, Perovskite phase

$Pb(Zr_{0.52}Ti_{0.48})O_3$ (PZT) sols were prepared by a modified sol-gel route using both solvents - acetic acid and stabilizer solution (n-propanol : 1,2-propanediol in the rate 10 : 1). The sols were deposited by spin-coating onto platinized Al_2O_3 or SiO_2/Si substrates. Results of SEM and XRD analyses confirmed, that the transformation of the amorphous PZT film to perovskite structure happened after sintering at 650°C. The mechanism of microstructure formation has described for morphologicaly different perovskite particle types in 1, 2 and 3-layered PZT thin films with thickness of 200-500 nm on used substrates. Three different PZT film microstructure types in dependence on the applied sol concentration were found. It was found, that the PZT/Pt/Al_2O_3 film microstructure at 1.0 M sol concentration was composed of two forms of perovskite particles, big rosette and irregular cuboidal particles. Small spherical particles and rosette structure were found in PZT/Pt/Si/SiO_2 films.

INTRODUCTION

Ferroelectric lead zirconate titanate $Pb(Zr_xTi_{1-x})O_3$ or (PZT) thin films have received much attention for applications such as sensors, microactuators and microelectromechanical systems (MEMS) [1,2]. For the preparation of perovskite PZT thin (<500nm) films chemical solution deposition (CSD) routes like sol-gel, chelate, Pechini and metallo-organic decomposition were used [3,4]. The first PZT precursor solution (sol) was prepared in 1985 by Budd et al. with solvent 2-methoxyethanol (sol-gel) [5], Yi et al. used acetic acid as a solvent with n-propanol or ethylene glycol as stabilizer [6]. PZT sols were deposited on different substrates (MgO, $SrTiO_3$, platinized silicon or alumina) by dip or spin-coating methods.

The various factors important to the use of sol-gel were discussed, including mechanisms for perovskite nucleation and growth or film thickness. The microstructure of the ferroelectric film is influenced by various processing conditions: the precursor chemistry, the sol concentration, nature of substrate, heat treatment and film thickness [7,8]. The sol-gel process has used to of deposit PZT films on different substrates in which the thickness of single sol-gel layer usually falls under 100 nm [9]. The deposition of thicker layers than this usually results in cracks and/or porosity formation. The required thickness is achieved by repeating the coating and heat treatment. The film thickness increases with rise in the concentration of PZT sols [10]. For lower concentration of PZT sol, the deposited film was a continous, while for high concentrations highly agglomerated structures were observed [11].

For PZT films processed at 650°C, the perovskite phase evolution consists of the following steps: phase separation in solution, pyrochlore crystallization, heterogenous nucleation and homogenous nucleation of perovskite [12,13]. X. J. Meng et al. [14] used a modified sol-gel method to prepare PZT thin film at low sintering temperature of 550°C. Sol-gel derived films typically have microstructures consisting of micrometer-sized particles clusters (rosettes) of perovskite surrounded by fine (<20 nm) pyrochlore in PZT films. In microstructures of the PZT film surface of other authors, particles of the perovskite phase with big rosette ~ 2-5 μm and columnar structure have been found on film cross-section on different substrate (Pt/Al_2O_3 or Pt/SiO_2/Si) [15,16]. The rosette structure is generally attributed to the perovskite phase, whereas the fine particle matrix consisted of Pb-deficient pyrochlore phase, $PbTi_3O_7$ or $Pb_2Ti_2O_{6+x}$ [17].

The present paper describes the preparation of PZT thin films using a modified sol-gel and spin-coating method from acetate based precursor sols. The effect of sol concentration with stabilizer solution (n-propanol:1,2-propanediol equals 10:1) on the microstructure of 1, 2 and 3-layered PZT thin films deposited on the Pt/Al_2O_3 or $Pt/SiO_2/Si$ substrates and mechanism of the microstructure formation are investigated.

EXPERIMENTAL

Preparation of PZT sols

PZT precursor solutions (sols) were prepared using the modified sol-gel synthesis according to the method in [18]. Lead acetate trihydrate $Pb(OAc)_2.3H_2O$ and zirconium acetylacetonate ($Zr(OR)_4$ were dissolved separately at a temperature of 80°C in glacial acetic acid AcOH in two closed flasks. The solutions were dehydrated at 105°C for 2 hours and after cooling to 80°C, they were mixed with titanium orthotetrabutylate $Ti(OR)_4$ in the required ratio of Pb:Zr:Ti = 1:0.52:0.48. After adding ethylene glycol at the temperature of 80°C, a yellow sol was formed. Finally, the basic 2.0M PZT sol was diluted with stabilizer solution (n-propanol:1,2-propanediol equals 10:1). The final sol concentrations after dilution were 1.5, 1.0 and 0.5M. The resulting orange solutions were transparent and remained stable at room temperature for several months.

Preparation and characterization of PZT thin films

Two different substrate types were applied for the PZT film deposition platinized alumina and silicon. Oxidized p-type silicon [100] single-crystal were used as substrates on which a Pt (50 nm) layer was sputtered as a bottom electrode. The Pt/Al_2O_3 and $Pt/SiO_2/Si$ substrates were spin-coated with the 0.5-1.5 M PZT sols at 2000 rpm for 30s followed by drying at 110°C for 3min and calcining at 400°C for 10min on a hot plate. The above coating-pyrolysis process cycle was repeated to obtain 1, 2 and 3-layered thin films. Finally, the films were crystallized through annealing at 650°C for 1hour in air to form the perovskite structure in the PZT thin films. Heating and cooling rates were ±5°C/min. The sol-gel preparation route for the PZT thin film and SEM surface micrographs of a 1-layer PZT thin film prepared from 1.0 M sol concentration on Pt/Al_2O_3 substrate are shown in Figure 1.

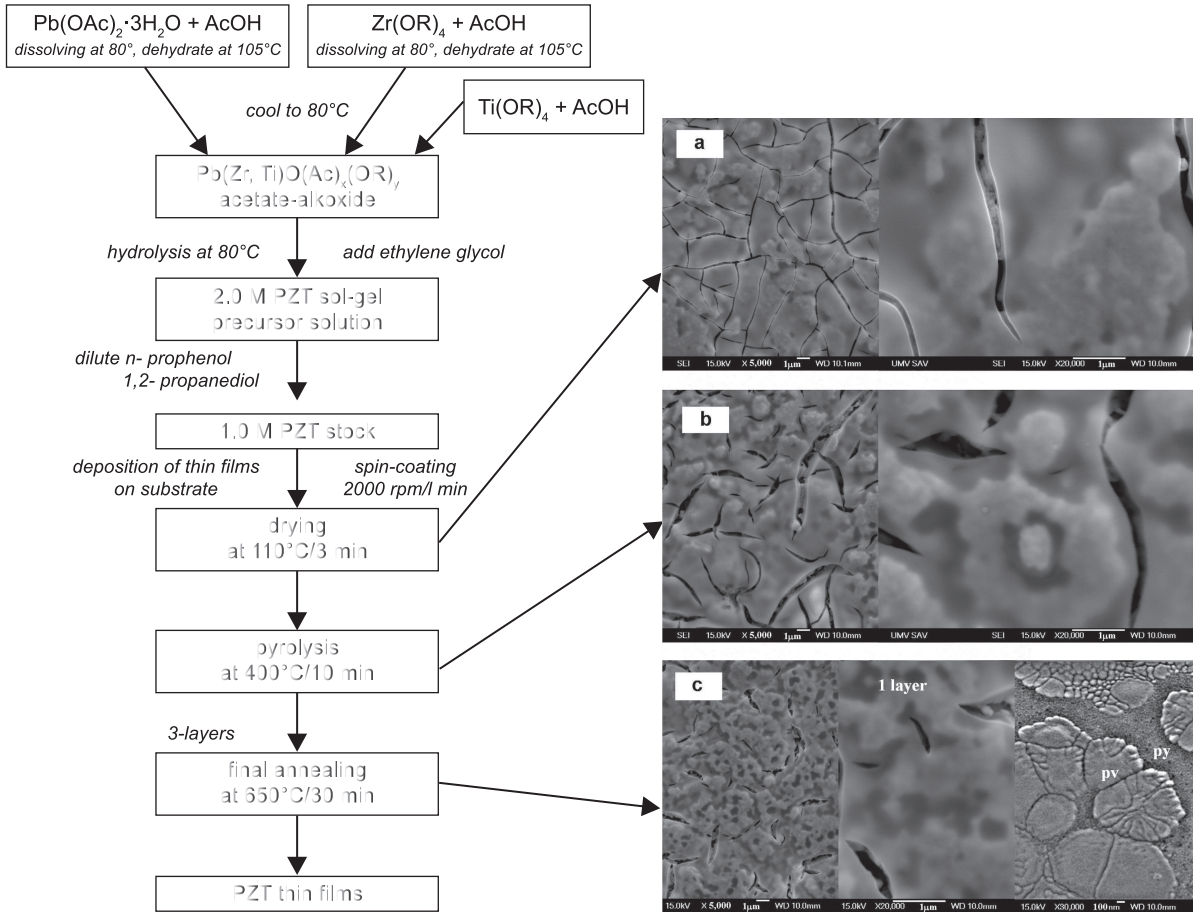

Figure 1. Sol-gel preparation route for the PZT thin film and SEM surface micrographs of 1-layer PZT thin film prepared from 1.0M sol concentration on Pt/Al_2O_3 substrate after processing - a) drying at 110°C, b) calcining at 400°C and c) sintering at 650°C.

The phase composition of PZT thin films was determined by X-ray diffraction analysis (XRD, Philips X´ Pert Pro) using CuK_a radiation. The surface and cross-section microstructures of PZT thin films were characterized using a scanning electron microscope (SEM, Jeol-JSM-7000F).

RESULTS AND DISCUSSION

PZT thin films deposited on Pt/Al_2O_3 substrates

1-layer PZT thin film surfaces prepared from 1.0M sol on Pt/Al_2O_3 substrate at various preparation stages are shown in Figure 1. In the micrographs, the xerogel-film (Figure 1a) and the amorphous PZT film (Figure 1b) with nano-sized irregular pores and holes can be seen. During the transformation of the film to perovskite PZT phase, the sols are first pyrolysed to pyrochlore phase. Since the PZT films were dried and calcined at relatively low temperatures of 110 and 400°C they contained more organic residuals. The organics probably inhibited the nucleation of perovskite particles. Figure 1c shows the crystallized 1-layer PZT film of 200 nm thickness after sintering at 650°C. The rosette structures of perovskite (pv) particles with average size ~ 100 nm and big rosettes ~1-5 μm were separated by a fine-grained phase ~8-20 nm (intermediate phase between amorphous pyrochlore (py) and crystalline perovskite). In the microstructures (Figure 1), the void formation arround the rosette particles with very sharp boundaries was observed. In the PZT thin films, py phases of $Pb_{0.75}Zr_{1.5}Ti_{0.5}O_x$ or $Pb_{1.2}Zr_{1.2}Ti_{0.8}O_x$ were observed [19-22]. In the microstructures, the void formation arround the rosette particles has been observed [23-24]. Rosettes had very sharp boundaries, which D. Van Genechten et al. interpreted in two different ways [25]. Firstly, sharp boundary is maintained during growth where a concentration gradient favours the formation of undulated interface and it forms rosette boundary. Secondly, conversion into pv phase from another crystalline phase such as py would require dissolution of the py nanocrystallites prior into incorporation as a part of the growing perovskite single crystal.

The XRD diffractogram and SEM micrograph of a 2-layered PZT thin film cross-section deposited on Al_2O_3/Pt prepared from 1.0M sol at 650°C are shown in Figure 2. The XRD diffractogram of the PZT film

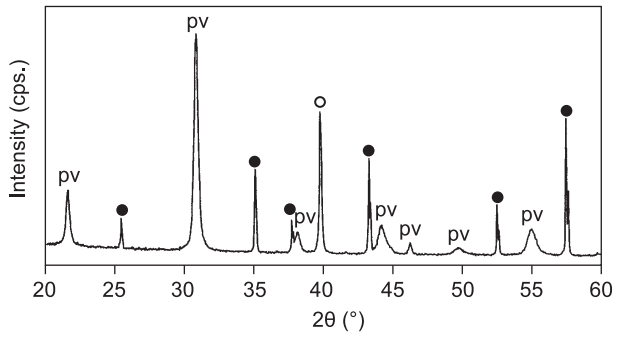

a) XRD diffractogram
(pv - perovskite phase, ● - Al_2O_3 substrate, ○ - Pt)

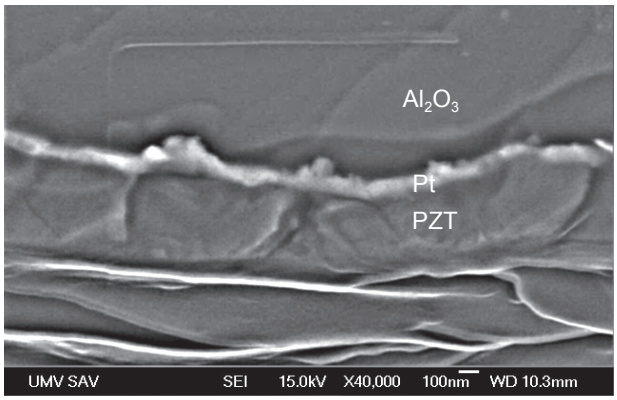

b) SEM cross-section micrograph

Figure 2. 2-layered PZT thin film prepared from 1.0M PZT sol and deposited on Pt/Al_2O_3 substrate after sintering at 650°C.

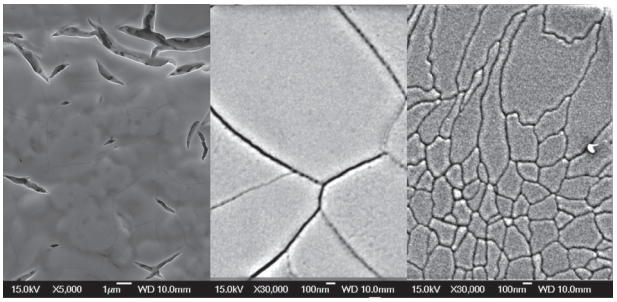

a) 2-layered PZT thin film

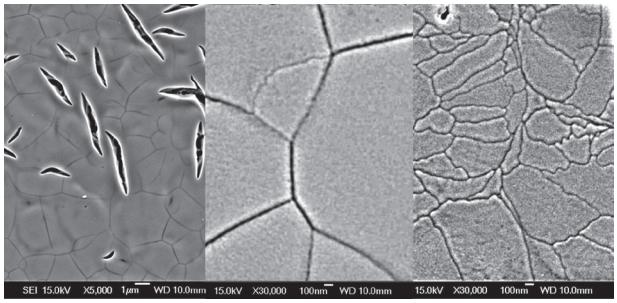

b) 3-layered PZT thin film

Figure 3. SEM surface micrographs of 2 and 3-layered PZT thin film prepared from 1.0M PZT sol on Pt/Al2O3 substrate after sintering at 650°C.

(Figure 2a) confirms the formation of fine perovskite $Pb(Zr_{0.52}Ti_{0.48})O_3$ phase (JCPDS 33-0784) with rhombohedral symmetry. The crystallite size in the film was arround ~29 nm (according to the Scherrer equation). The columnar structure of pv particles of 350 nm thickness is visible in 2-layered thin PZT film cross-section prepared from 1.0M sol (Figure 2b).

In Figure 3, two types perovskite particle in microstructure of 2-layered (Figure 3a) and 3-layered (Figure 3b) PZT thin film can be seen: large cuboidal particles of ~ 0.2 -1.5 μm and small particles of ~ 50-120 nm size with 30 nm pores. With the increase of coating cycles, large particles and few voids become visible in the microstructure (Figure 3b) at a film thickness of 450 nm.

In Figure 4, a effect of the molarity of the sols on the pore structure (Figures 4a,b) and number of cracks (Figures 4c,d) in 2 and 3-layered PZT thin films can be observed. Films prepared from variously concentrated sols on Pt/Al_2O_3 substrates differ in crack density after sintering at 650°C. The film prepared from 0.5M sols had less cracks and pores than films prepared from 1.5M sols. The increase of the precursor sol concentration results in the growth of particles. 2 and 3-layered PZT thin films prepared at 650°C were composed of large equiaxed particles (~ 1.5 μm) and small cuboidal particles (~ 80-120 nm). The optimal molar concentration from the point of view of 2 and 3-layered PZT thin film microstructures was 1.0M (Figures 3a,b).

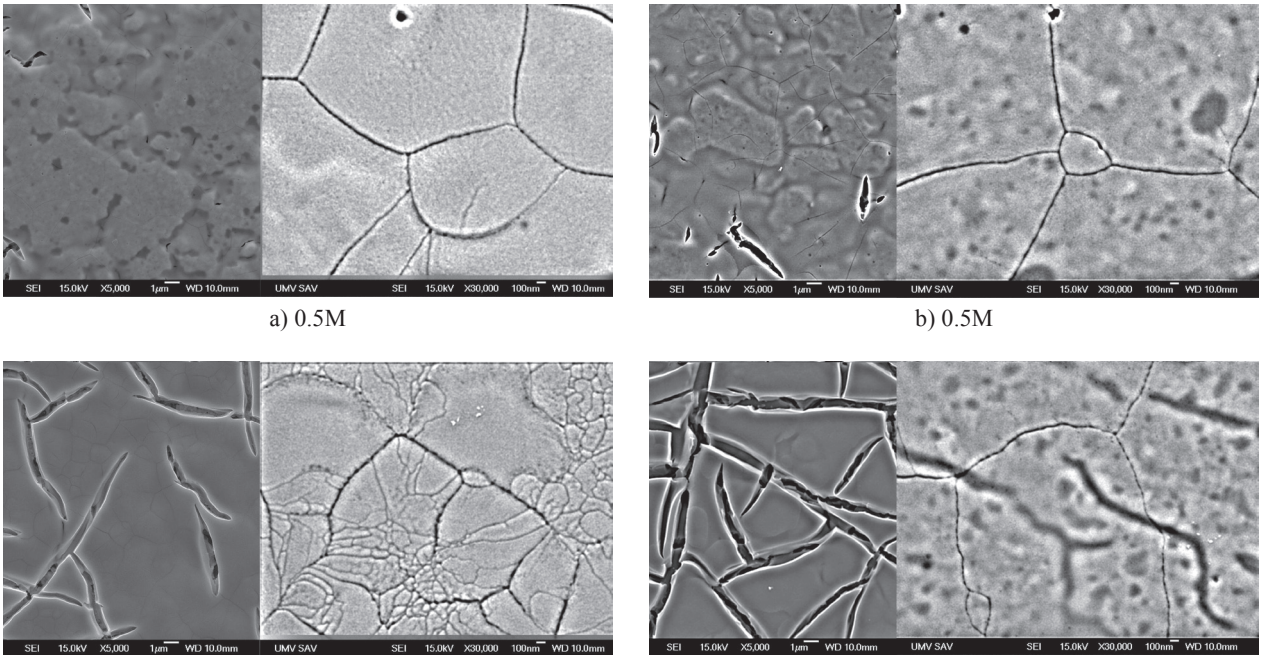

a) 0.5M b) 0.5M

c) 1.5M d) 1.5M

Figure 4. SEM surface micrographs of 2 and 3-layered PZT thin film prepared from different molar concentration of sols on Pt/Al_2O_3 substrate after sintering at 650°C.

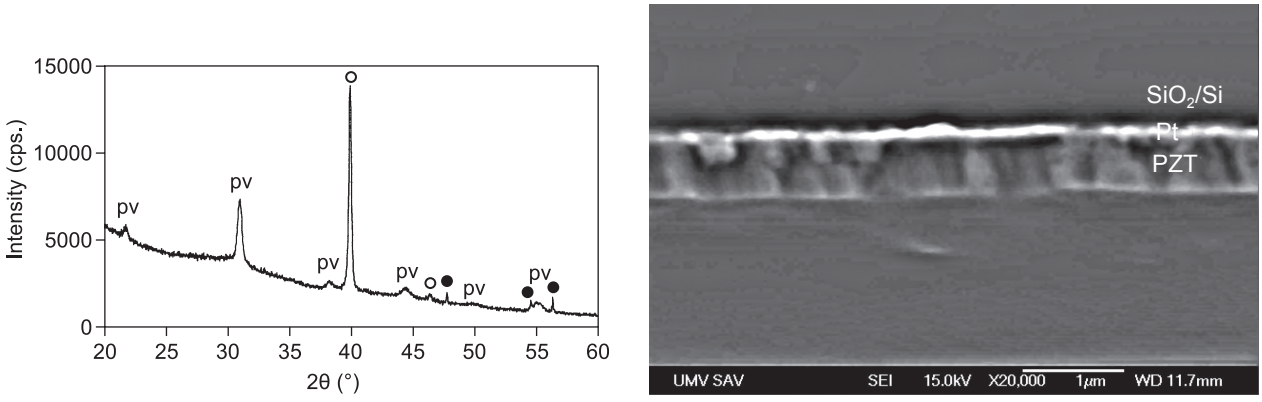

a) XRD diffractogram
(pv - perovskite phase, ● - SiO_2/Si substrate, ○ - Pt)

b) SEM cross-section micrograph

Figure 5. 2-layered PZT thin film prepared from 1.0M PZT sol and deposited on $Pt/SiO_2/Si$ substrate after sintering at 650°C.

PZT thin films deposited on $Pt/SiO_2/Si$ substrates

The XRD diffractogram and SEM cross-section micrograph of a 2-layered PZT thin film deposited from 1.0M sol on $Pt/SiO_2/Si$ prepared at 650°C are shown in Figure 5. In Figure 5a, an XRD pattern close to pure perovskite (pv) phase $Pb(Zr_{0.52}Ti_{0.48})O_3$ (JCPDS 33-0784) with rhombohedral symmetry was found. The crystallite size in the pv phase was about ~20 nm. SEM cross-section micrograph of a 2-layered PZT thin film with the columnar microstructure of the coating is visible in Figure 5b. The thickness of 2-layered PZT films on the $Pt/SiO_2/Si$ substrate was 400 nm. Particle nucleation starts from the Pt electrode/PZT interface in the first layer (250 nm) and the subsequent layer inherits the morphology from the previous layer.

In Figure 6, SEM surface micrographs of 1, 2 and 3-layered PZT thin films of thickness (250, 400 and 500 nm) prepared from 1.0M sol on $Pt/SiO_2/Si$ substrate after sintering at 650°C are shown. The 1-layer PZT film surface (Figure 6a) is smooth and void-free without rosette structure. The spherical pv particles size equals ~40-100 nm. Similar spherical particles of pv PZT phase were shown in PZT films in [26]. In [27], the PZT thin films prepared on $Pt/Ti/SiO_2/Si$ substrates by the sol-gel method and sintered at 650°C were composed of coarse particles without rosette structure. Increase the number of coating cycles affect the size of particles and voids in the films. Non-uniform films with rosette structured particles (Figures 6b,c) can be visible in microstructures of 2 and 3-layered PZT films whereas the average rosette size was 1-2 μm. Rosette particles consist of smaller spherical and cuboidal particles. In the microstructure of 2-layered PZT films on $Pt/SiO_2/Si$ substrate spherical particles ~0.2-1.0 μm (Figure 6b) were found and cuboidal particles in rosettes with size of 80 nm in 3-layered PZT thin film were observed, respectively. Similar surface morphology and rosette pv phase formation with diameter of 5-15 μm were observed by Z. J. Wang et al. [28]. The matrix regions between rosettes were identified to be fine py phase, which could not be detected by XRD analyses. In [29] PZT thin films on $Pt/SiO_2/Si$ substrates sintered at 600°C were composed of two circular pv rosettes developed from the surrounding nanoscale py matrix. In [30-32], the surface morphologies of PZT thin films on $Pt/Ti/SiO_2/Si$ substrate yielded rosette structure which consisted of large (~1 μm) spherical particles.

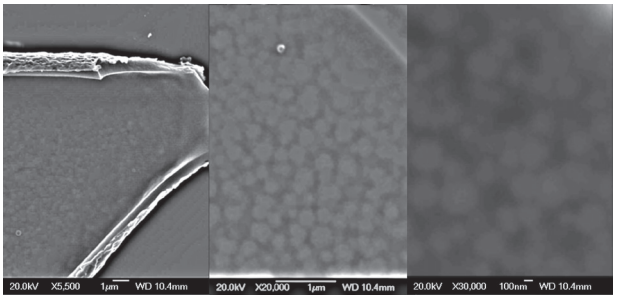

a) 1-layer

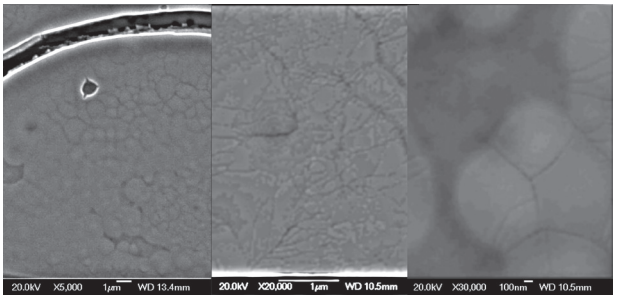

b) 2-layers

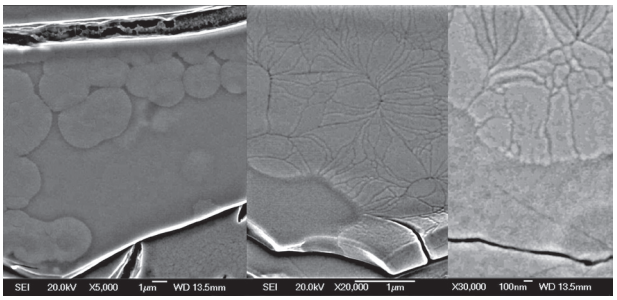

c) 3-layers

Figure 6. SEM micrographs of surface of thin PZT film prepared from 1.0M PZT sol on $Pt/SiO_2/Si$ substrate after sintering at 650°C.

Mechanisms for perovskite nucleation and growth or film thickness

The probably microstructure evolution can be derived from the comparison of observed individual microstructures in dependence on the applied sol concentration. The microstructure of 1-layer PZT film in Figure 1c (1.0M sol concentration) is composed of finer and separate pv particles with rosette morphology and high pore fraction. On the other hand, particles of pv phase in Figure 4a (0.5 M sol concentration), where the coating contains the same amount of PZT phase, have a more spherical shape with smooth surface without characteristic rosette structure and markedly lower pore portion. It is clear from the above, that a higher number of nuclei is created by fast calcination of more concentrated PZT sols. Individual nuclei form discrete crystallization centers differ from each other by activity and almost of them grow uniformly until they touch with boundaries. As consequence of volume changes and matter transfer during two physical different processes - firstly, the thermal degradation of organic compounds, mutual interaction and connecting of created transition oxidic compounds and secondly, sintering and recrystallization of oxidic phases - the substrate surface is not uniformly coated by pv phase. The first layer created by the decomposition of 0.5M sol includes distant pv particles where ion movement on the substrate surface by diffusion is practically impossible because of the discontinuous

PZT film. In this case, the formation of particles of rosette shape is restricted. The above mechanism has to be distinguished from that in the second PZT layer on Pt/Al_2O_3 substrate, where particles grow on first created nuclei or nanometric particles. Since the fraction of nuclei for crystallization of PZT phase in the film is lower in the case of 0.5M sol than film created from more concentrated sols (2-3 times higher), the particles have sufficient area for their growth to larger dimensions until they will touch by its boundaries and a more continuous and smooth layer with uniform particles size is created. The second layer deposited from 1.0M sol on the first uncontinuous layer composed of rosette pv particles separated by narrow channels of the py phase causes the growth and coalescence of origin rosette particles into the big particles of micrometric size. On the other hand, this causes the formation of new nuclei or pv phase particles by the transformation of py phase after interaction with the new PZT sol-film. This is probably the mechanism for the formation of the microstructure with two morphological different pv particle types. It is clear from Figure 4c,d that the number of nuclei and crystallization centers is sufficient in the coating created from the 1.5M sol for the preservation of finer microstructure with the high fraction of irregular pv nanometric particles. The recrystallization into larger perovskite particles can be only observed at adjacent particles with significantly different surface activities (at contact between low- and high- angle boundaries).

On the $Pt/SiO_2/Si$ substrate, the formation of morphologically different spherical uniformly distributed nanometric PZT particles on substrate surface from 1.0M sol in comparison with Pt/Al_2O_3 substrate is visible. The subsequent deposition of the second PZT layer causes the growth of spherical particle size (2-3 times), which is stopped by mutual particle boundary contact. However, is not observed particle sintering to large continous areas and the number of crystallization centers is almost unchanged. This fact influenced the character of microstructure after deposition of the third PZT layer. In the microstructure in Figure 6b, the initial mutual segregation of larger particle agglomerates is observable as the result of the formation of new boundary between agglomerates by particle sintering. In the 3-layered coating, the apparent separation of spherical pv particles agglomerates with rosette morphology composed of the high fraction of fine irregular pv particles has been visible after recrystallization and sintering.

CONCLUSIONS

The mechanism of the microstructure formation with morphologicaly different perovskite particles in PZT thin films was described. The morphology of the PZT film after crystallization at 650°C was influenced by the substrate. In the microstructures of the 1-, 2- and 3-layered $PZT/Pt/Al_2O_3$ or $PZT/Pt/Si/SiO_2$ thin film surfaces, rosette, cuboidal or spherical perovskite phase particles with columnar structure on film cross-section were observed. A more porous structure was formed at low sol concentration and the number of cracks in films rises with the sol concentration (various amounts of stabilizer solution).

An effect of coating thickness on the particle morphology in the PZT thin films on both substrates was found. The 1-layer $PZT/Pt/Al_2O_3$ thin film (of 200 nm thickness) microstructure with micrometer-scale rosette particles differs from 1-layered $PZT/Pt/Si/SiO_2$ thin film (of 250 nm thickness) microstructure composed of small spherical particles (~ 40-100 nm).

In the 2- and 3-layered $PZT/Pt/Al_2O_3$ thin films (of 350 and 450 nm thickness respectively), two forms of perovskite phase particles were observed: big rosette structures (~ 1-5 μm) composed of small cuboidal particles (~50-120 nm) with 30 nm pores and equiaxed cuboidal particles (~ 0.5-1.5 μm). Spherical particles (~ 0.2-1.0 μm) and rosette structures of perovskite phase with small cuboidal particles were found in the 2- and 3-layered $PZT/Pt/Si/SiO_2$ thin films (of 400 and 500 nm thickness).

A strong effect of the sol concentration on microstructure evolution was found and a correct choice of the sol concentration allows the formation of the film microstructure required.

Acknowledgement

This work was supported by the Grant Agency of the Slovak Academy of Sciences through project No. 2/0024/11.

References

1. Chen B.H., Huang C.L., Wu L.: Thin Solid Films *441*, 13 (2003).
2. Wang D.G., Chen C.Z., Ma J., Liu T.H.: Appl. Surf. Sci. *255*, 1637 (2008).
3. Schwartz R.W.: Chem. Mater. 9, 2325 (1997).
4. Fukushima J., Kodaira K., Matsushita T.: J. Mater. Sci. *19*, 595 (1984).
5. Budd K.D., Dey S.K., Payne D.A.: Brit. Ceram. Soc. Proc. 36, 107 (1985).
6. Yi G., Wu Z., Sayer M.: J. Appl. Phys. *64*, 2717 (1988).
7. Sun D., Rocks S.A., Wang D., Edirisinghe M.J., Dorey R.A.: J. Eur. Ceram. Soc. *28*, 3130 (2008).
8. Haiyan H.: Current Opinion in Solid State Mater. Sci. *12*, 19 (2009).
9. Zhang Q., Corkovic S., Shaw C.P., Huang Z., Whatmore R.W.: Thin Solid Films *488*, 258 (2005).
10. Whatmore R.W., Zhang Q., Huang Z., Dorey R.A.: Mater. Sci. Semicond. Proc. *5*, 65 (2003).
11. Dobbelaere C.D., Hardy A., Haen J.D., Van den Rul H., Van Bael M.K., Mullens J.: J. Eur. Ceram. Soc. *29*, 1709 (2009).

12. Chen S.Y., Chen I.W.: J. Amer. Ceram. Soc. *77*, 2332 (1994).
13. Huang Z., Zhang Q., Whatmore R.W.: J. Appl. Phys. *85*, 7355 (1999).
14. Meng X.J., Cheng J.G., Li B., Guo S.L., Ye H.J., Chu J.H.: J. Crystal Growth *208*, 541 (2000).
15. Pintilie L., Boerasu I., Gomes M.J M., Pereira M.: Thin Solid Films *458*, 114 (2004).
16. Pérez J., Vilarinho P M., Kholkin A. L., Almeida A.: Mater. Res. Bull. *44*, 515 (2009).
17. Hwang K.S., Manabe T., Nahagama T., Yamaguchi I., Kumagai T., Mizuta S.: Thin Solid Films *347*, 106 (1999).
18. Brunckova H., Medvecky L., Briancin J., Saksl K.: Ceram. Int. *30*, 453-460 (2004).
19. Uhlmann D.R., Teowee G., Boulton.M., Motakef S., Lee S.C.: J. Non-Crystalline Solids *147&148*, 409 (1992).
20. Shturman I., Shter G.E., Etin A., Grader G.S.: Thin Solid Films *517*, 767 (2009).
21. Gong W., Li J.F., Chu X., Gui Z., Li L.: Acta Mater. *52*, 2787 (2004).
22. Jeong Y.S., Lee H.U., Kim J.P., Kim H.G., Jeong S.Y., Cho C.R.: Current Appl. Phys. *9*, 115 (2009).
23. Dunn S., Whatmore R.W.: Intergrated Ferroelectrics *38*, 39 (2001).
24. Labardi M., Allegrini M., Leccabue F., Wats B.E., Ascoli C., Frediani C.: Solid State Communications *91*, 59 (1994).
25. Van Genechten D., Vanhoyland G., Haen J.D., Johnson J., Wouters D.J., Van Bael M.K., Van den Rul H., Mullens J., Van Poucke L.C.: Thin Solid Films *467*, 104 (2004).
26. Zhu C., Yong Z., Chentao Y., Bangchao Y.: Appl. Surface Sci. *253*, 1500 (2006).
27. Jiwei Z., Xi Y., Liangying Z.: Ceram. Int. *27*, 585 (2001).
28. Wang Z.J., Aoki Y., Yan L.J., Kokawa H., Maeda R.: J. Crystal Growth *267*, 92 (2004).
29. Ulcinas A., Souni M.E., Snitka V.: Sensors Actuators B *109*, 97 (2005).
30. Lee C., Spirin V., Song H., No K.: Thin Solid Films *340*, 242 (1999).
31. Bhaskar A., Chang T.H., Chang H.Y., Cheng S.Y.: Appl. Surf. Sci. *255*, 3795 (2009).
32. Kayasu V., Ozenbas M.: J. Eur. Ceram. Soc. *29*, 1157 (2009).